Available online at www.sciencedirect.com
SCIENCE DIRECT®
Nuclear Instruments and Methods in Physics Research A 541 (2005) 15–20
NUCLEAR INSTRUMENTS & METHODS IN PHYSICS RESEARCH Section A
www.elsevier.com/locate/nima

Beam splash effects on ATLAS silicon microstrip detectors evaluated using 1-w Nd : YAG laser

K. Hara[a,*], T. Kuwano[a], G. Moorhead[b], Y. Ikegami[c], T. Kohriki[c], S. Terada[c], Y. Unno[c]

[a]*Graduate School of Pure and Applied Sciences, University of Tsukuba, 1-1-1 Ten'nodai, Tsukuba, Ibaraki 305-8571, Japan*
[b]*School of Physics, University of Melbourne, Parkville Victoria 3010, Australia*
[c]*High Energy Accelerator Research Organization (KEK), Oho 1-1, Tsukuba, Ibaraki 305-0801, Japan*

Available online 5 February 2005

Abstract

On an incident of accelerator beam loss, the tracking detector located close to the beam line is subjected to receive intensive radiation in a short period. We used a 1-W focused Nd : YAG laser and simulated the effects on the ATLAS microstrip detector. The laser corresponds to intensity of up to 1×10^9 mips/pulse with a pulse width of about 10 ns. We observed breaks on Al strips on extreme conditions, depending on the laser intensity and bias voltage applied to the silicon sensor. The break can be interpreted as the oxide breakdown due to a large voltage locally created across the oxide by the intensive signal charges. The robustness of the Semiconductor Tracker (SCT) module including readout ASICs is also evaluated.

PACS: 29.40.Gx; 29.40.Wk

Keywords: Silicon microstrip detector; ATLAS SCT; YAG laser; Beam loss; Beam splash; Breakdown

1. Introduction

The LHC will circulate approximately 10^{11} protons per bunch and collide them at a frequency of 40 MHz. The detector, especially tracking detector located close to the beampipe, must be robust against possible beam loss where the detector may receive intensive particles in a short period. According to a scenario and simulation, the CMS group predicted that a loss of 10^9 proton/cm^2 within 260 ns should occur at least once a year and conducted a testbeam measurement [1]. They have shown that the CMS Si tracker survives a beam of 7×10^{10} protons spread over $10 \times 3\,\text{cm}^2$. The survival is explained stating that the large number of free carriers created by the intensive radiation effectively reduces the

*Corresponding author.
E-mail address: hara@hep.px.tsukuba.ac.jp (K. Hara).

0168-9002/$ - see front matter © 2005 Published by Elsevier B.V.
doi:10.1016/j.nima.2005.01.033

electric field across the bulk and the bias voltage is not sustained. This mechanism of electric field breakdown is pointed out in Ref. [2]. The external RC bias network supplies quickly the charge to recover from the breakdown. Therefore the feature of the electric field breakdown should depend on the values of R and C [2].

In the studies reported in Refs. [1,2], the silicon microstrip detectors are found to be safe in their test conditions. We used a Nd:YAG laser of 1064 nm, as in Ref. [2], to simulate the passage of charged particles. The laser power we used was 1 W with the intensity continuously reducible by orders of magnitude. The laser pulse width is short (6 ns FWHM) and is focused to 8 μm in diameter, which are to be compared with 1 μs and 10 μm in diameter in Ref. [2].

ATLAS Semiconductor Tracker (SCT) barrel modules [3] are used in this study. The sensors are p-on-n single-sided microstrips, fabricated by Hamamatsu Photonics (HPK). The dimensions of the sensor are $63.56 \times 63.96 \times 0.285\,\mathrm{mm}^3$. The sensor has 768 readout AC-coupled Al electrodes of 22 μm width at a pitch of 80 μm. The implant electrodes of 16 μm width are grounded via 1.25 MΩ poly-silicon bias resistors, with the backplane being biased. Each module has four sensors glued back-to-back on to a baseboard. The two sensors on the same side are wirebonded together, having effectively 124 mm long strips. The signals from the both sides, 1536 channels in total, are read out with 12 binary readout ASICs, ABCD3T chips [4], which are mounted on a Cu-polyimide hybrid [5]. The sensors will be biased up to between 350 to 500 V, depending on irradiation, thus on the distance from the collision point. The hybrid is equipped with 50 nF capacitance between the backplane and ground, and 5.1 kΩ series resistance to the backplane.

2. Laser system and intensity calibration

Because the energy of Nd:YAG laser is just above the Si band-gap energy of 1.12 eV, most of the laser light penetrates the Si sensor and the energy is liberated, if absorbed, it will be almost uniformly along the path. The laser system [6] consists of a laser head (Spectra-Physics Model S12-1060), intensity controls and a focusing lens. We have two independent intensity control systems, Glan polarizer and neutral-density (ND) filters. Since the laser is 100% polarized, the intensity can be varied by rotating the angle of the polarizer. There are two pairs of "thick" and "thin" ND filters located downstream the Glan polarizer. The laser aperture is then defined by XY windows and the laser is focused with a microscope (×50 magnification). The laser with no ND filter is intensive enough to evaporate Al electrodes.

The laser intensity was calibrated using a real ATLAS SCT module. The signal with all ND filters inserted was read out via an SCT–DAQ system, and is calibrated with ABCD3T chip gain (55 mV/fC) [7]. The transparency curve of the Glan polarizer in terms of the rotation potentiometer was then obtained by choosing the laser spot size so that the intensity is within the measurement range of the ABCD3T (less than 680 mV). After this procedure, setting the Glan polarizer at a reduced intensity, one of thin or thick ND filters is taken out to calibrate their transparencies. The intensity at the different setting was calculated from the Glan polarizer transparency curve and transparencies of the ND filters.

The laser was operated at 1 kHz: the intensity is constant up to 1 kHz then decreases gradually [7]. Fig. 1 plots the calculated laser intensity in terms of number of mips per pulse and the expected signal current. Here we assumed that 2×10^4 holes are collected per mip as the signal. The detector currents in the figure were measured with an amperemeter. Although there exists a discrepancy up to a factor of two at lower intensities, the two curves are in reasonable agreement. The maximum laser intensity is 1×10^9 mips/pulse.

3. Robustness of the HPK microstrip sensor

3.1. Creation of break in Al electrodes

We observed that the Al electrode of the microstrip sensor breaks above certain bias voltage and laser intensity. Fig. 2 is a typical trace

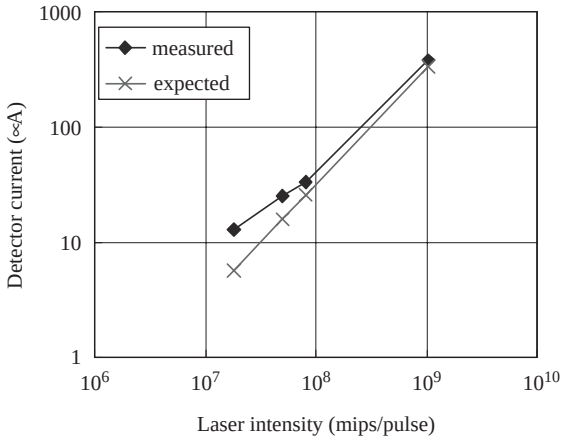

Fig. 1. Calibration of the laser intensity. The expected detector current (see text) and the measured current are in reasonable agreement, verifying the reliability of the laser intensity calibration in terms of number of mips per laser pulse.

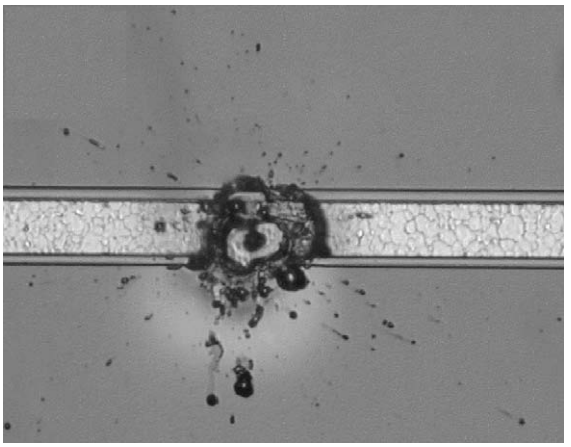

Fig. 2. Hole is created on the Al electrode at 500 V bias voltage and 1×10^8 mips. The laser is injected about 30 μm off the Al electrode. The Al electrode is 22 μm wide.

of the break. Note that the laser, confined in a diameter of 8 μm, is injected just aside the Al not to hit it directly. Since the laser at highest intensity would evaporate the Al if it hits the Al directly, this procedure is carefully completed so that the present study is not sensitive to the damage specific to the laser. Note also that the damage trace shown in the figure is apparently different from the evaporation trace that would be created by the laser hitting directly.

Fig. 3 shows the probability to create such breaks as a function of the bias voltage. The histograms are shown for three different laser intensities, $0.6 \times 10^7, 2 \times 10^7$ and 8×10^7 mips/pulse. Most of the samples, except only one, are good to 500 V for 0.6×10^7 and 2×10^7 mips/pulse. The laser was pulsed at 1 kHz and for a duration up to 10 s. For 8×10^7 mips/pulse, however, some strips broke at 350 V and the probability reached about 50% at 450 V. Most of the breaks were created within 1 s, or by the first shot when the laser was operated at 1 Hz, but some required a few seconds.

At lower bias voltages of 150 and 200 V, no breaks were created up to the highest laser intensity, 1×10^9 mips/pulse, and up to the order of 10^4 pulses we injected.

We note that Al breaks of the HPK sensors were always initiated at the point closest to the laser injection point. Although the study was not systematic, we also tested a CiS sensor of the same ATLAS design. The CiS sensor is found to break typically at 350 V for 0.6×10^7 mips. Distinctive difference is that the break was initiated on the nearby Al electrode but at a point somewhat away (30 μm and 0.5 mm, two samples) from the laser injection point. We interpret the above as that the HPK sensors were broken at the point where the electric field is maximum while the CiS sensors break where the oxide layer has some weak point.

3.2. SPICE simulation

In order to understand the reason for the breaks, we modeled the microstrip detector and external bias RC network in a SPICE simulation. The model used in the simulation is illustrated in Fig. 4, where the sensor parameters are given in the figure caption. A triangular shaped current source with 10 ns base width was generated at a point located 5 cm apart from the readout end. The detector bias is 500 V. Fig. 5 shows a time evolution of voltages on the implant and Al electrodes at the point where the current was generated, and at 1.5 mm apart from the current

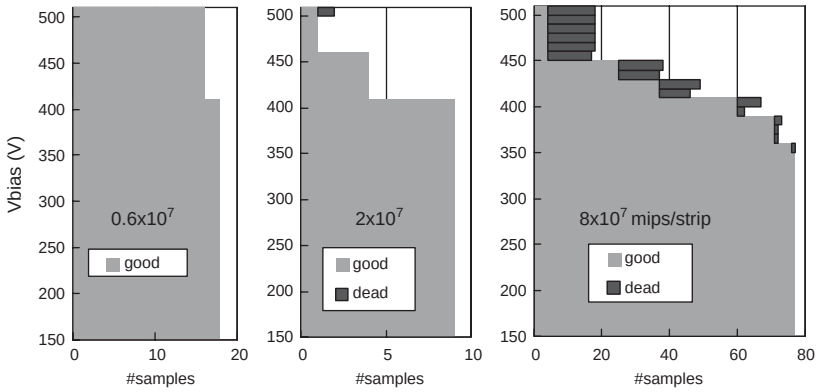

Fig. 3. Probability of hole creation as a function of the bias voltage. Filled (open) histogram represents the number of passed (failed) samples. The data are shown for three laser intensities.

Fig. 4. SPICE model of the microstrip detector: Al resistivity (R_{Al}) 15 Ω/cm, implant resistivity (R_i) 20 kΩ/cm, equivalent ASIC resistance (R_{ic}) 1 kΩ, bias resistor 1.25 MΩ, coupling capacitance (C_{cp}) 25 pF/cm, bulk capacitance (C_{bk}) 2.5 pF/cm, interstrip capacitance 5 pF/cm, finite backplane resistance (R_{bk}) 10 Ω (overestimated to see effects), bias voltage network $R = 5.1$ kΩ, $C = 50$ nF.

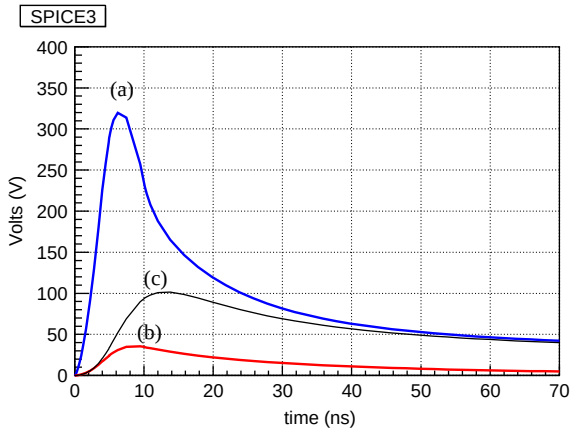

Fig. 5. Evolution of (a) implant and (b) Al electrode voltages at the signal source, and (c) the implant voltage 1.5 mm away (SPICE simulation).

source. Although effects such as space charge must be taken into account, the generated charge corresponds to 5×10^6 mips. The simulation results in different peak voltages, creating a large voltage difference across the oxide layer at the injection point. Also the peak voltage at the implant decreases with the distance from the signal source.

Contrary to the implant voltage increase, the bias voltage stays almost constant. The bias voltage drop can occur only through R_{bk} and is small, since the generated charge, 16 nC, is far below the charge 25 μC stored in the external capacitor. In the electric field breakdown model [2], the large signal charge pulls down the bias voltage and pulls up the implant voltage. Such a change in the bias voltage should be seen only for $>10^9$ mips in our external circuit. In our simulation, only the implant voltage is pulled up due to the smaller bulk capacitance and larger implant resistance compared with the coupling capacitance and Al resistance. The implant resistance induces also a local voltage difference along the electrode, as shown in the figure, peaking the oxide voltage at the point where charges are created.

The HPK coupling capacitors are specified to be durable up to 100 V. We tested the coupling capacitors of the HPK sensor applying DC voltages across. The break voltages were found to be about 190 V and were very uniform. The present simulation describes qualitatively well that the coupling capacitors of the HPK sensors can

Table 1
Robustness of the SCT modules. The functionality is categorized as normal ("OK"), completely no response ("dead"), or some bad channels ("?"), as a function of the laser intensity in mips/pulse

Bais voltage (V)	2×10^7	4×10^8	7×10^8	1×10^9	comment
150	OK	OK	OK	OK	
200	OK	OK	?	Dead	
200	OK	OK	?	?	
200	OK	OK	OK	Dead	
400	OK	OK	OK	OK	laser spread over 3 strips

The laser (8 μm in diameter) is focused to one strip except for the one at the bottom where the laser was spreaded over three strips.

break at the point where a large current is generated. Quantitative description, however, requires a simulation which takes space-charge effects into account and detailed data concerning the coupling capacitor durability against voltages applied in a short period of about 10 ns.

4. Robustness of the SCT modules

We observed that the chip connected to the electrode lost the entire functionality whenever the Al electrode was broken. It is found that the ASIC input circuit trace connected to the broken electrode got colored and the trace sparked toward the power lines located underneath.

The study is extended to search the conditions where the sensor electrodes are not broken but the ASIC is damaged. Although statistically limited, the results are summarized in Table 1. The functionality of the module was evaluated using the ASIC test pulse. The module with 150 V bias functioned normally, giving proper gain and noise values, up to 10^9 mips/pulse. The modules at 200 V bias were completely dead at 10^9 mips/pulse. At lower intensities with 200 V bias (marked ? in the table), several channels around the laser injection point became sick, providing larger noise values.

The above results are for the case where the laser was focused at one strip. Since the local electric field must be dependent on the laser spot size, we enlarged the spot to cover three strips. In this situation, the module was found to function properly at much higher bias of 400 V up to 10^9 mips/pulse. The Al electrodes broke at 10^9 mips/pulse at around 430 V, so the study at higher voltage was not possible.

5. Conclusions

Using a 1-W YAG laser, we have evaluated the robustness of the ATLAS microstrip sensor and of module against possible incident of accelerator beam loss. The Al electrodes of the microstrip sensors can be broken at high biases and large signal current. The break typically occurs at 350 V for 10^8 mips/pulse if the laser is focused at one strip. The reason can be interpreted as the oxide breakdown. The ASIC chip can be dead at 10^9 mips/pulse at 200 V bias. If the laser spot is expanded to three strips, the module at 400 V bias functions properly up to 10^9 mips/pulse.

If we take the same robustness requirement of the CMS Si tracker, 10^9 proton/cm^2 in 260 ns, our last condition, 10^9 mips/(0.2 mm)^2 in 6 ns (FWHM), is by far severe in view of the electric field strength. In order to assure that the field breakdown occurs within a few ns to quench the voltage increase in the case of a beam loss of much larger number of particles, the finite backside resistance R_{bk} must be kept below a few 10 mΩ; a 50 nF capacitor and R_{bk} determine the time constant. Since such a small resistance is not realized reasonably, we must foresee that the field breakdown follows after a substantial increase in the local voltage across the coupling capacitors.

As a conclusion, the ATLAS SCT microstrip detector can be damaged due to accelerator beam loss, but only in very extreme conditions

where the detectors are fully biased exceeding about 400 V and the beam of exceeding 10^9 particles is focused to a few strips, or in equivalent conditions where the generated charges create a large enough voltage to break the oxide layer of the microstrips.

Acknowledgements

We would like to thank the members of the SCT group, especially the module group, who inspired us to conduct the present study.

References

[1] M. Fahrer, et al., Nucl. Instr. and Meth. A 518 (2004) 328.
[2] T. Dubbs, et al., IEEE Trans. Nucl. Sci. NS-47 (6) (2000) 1902.
[3] K. Kondo, et al., Nucl. Instr. and Meth. A 485 (2002) 47; ATLAS Inner Detector Technical Design Report, CERN/LHCC 97-16, CERN/LHCC 97-17, 1997.
[4] W. Dabrowski, et al., Proceedings of the Sixth Workshop on Electronics for LHC Experiments, CERN/LHCC/2000-41, p. 115.
[5] Y. Unno, et al., Nucl. Instr. and Meth. A, this issue.
[6] Y. Unno, et al., Nucl. Instr. and Meth. A 383 (1996) 238.
[7] K. Hara, et al., Nucl. Instr. and Meth. A, this issue, doi:10.1016/j.nima.2005.01.048.